Theory of Magnetic Transmission Lines

J. A. Brandão Faria, *Fellow, IEEE*, and Miguel P. Pires

***Abstract*—This paper presents, for the first time, the frequency-domain theory of magnetic transmission lines, i.e., transmission lines where electromagnetic energy guidance is assured by means of two magnetic-flux carrying parallel magnetic wires, as opposed to the ordinary situation of two current carrying parallel electric wires (an electric transmission line). Propagation equations for the fundamental quasi-TEM mode are established and solved. Wave parameters are analyzed. A transmission matrix is described.**

***Index Terms*—Electromagnetics, energy guidance, magnetic transmission line (MGTL), transmission-line theory.**

I. Introduction

TRANSMISSION-LINE theory is one of the oldest topics in electromagnetics, with applications spanning from power systems to microwave systems. The subject is usually dealt with considering a pair of parallel electric wires, carrying longitudinal currents, immersed in an insulating dielectric medium. In the case of good conducting wires, the quasi-TEM approach is ordinarily utilized. The literature on electric transmission lines (ELTLs) is hyper abundant. On the contrary, magnetic transmission lines (MGTLs), which employ a pair of parallel magnetic wires of high permeability, have received very scarce attention. The subject is addressed in a paper dedicated to contactless energy transfer [1], in an old 1968 patent [2], and also in a very recent pending patent [3].

In [1] it is shown, from Maxwell's equations, that the instantaneous power across a transverse section of an MGTL is given by $p = u\, d\phi/dt$, where u is the magnetic voltage between magnetic wires and ϕ is the magnetic flux carried by the wires. The Kerns patent [2] is concerned with harmonics suppression in a voltage transformer that is provided with conductive membranes set in place to attenuate frequencies above 60 Hz. The Faria patent [3] points toward MGTL applications in the terahertz band.

This paper is organized into eight sections, the first of which is introductory. Section II is dedicated to the formulation of the problem; ordinary results for ELTLs are briefly reviewed; the duality between electric and magnetic concepts pertaining to transmission-line theory is presented. The propagation equations governing MGTLs are established in Section III. The frequency-domain solution of MGTL propagation equations is worked out in Section IV. Section V is devoted to the analysis of the sending and receiving ends of the MGTL structure. Approximate expressions of the wave parameters (propagation constant and characteristic impedance) of the MGTL are obtained in Section VI considering the case of small losses. Sections VII and VIII are devoted to discussion and conclusions.

Manuscript received May 29, 2012; accepted July 05, 2012. Date of publication August 13, 2012; date of current version September 27, 2012. This work was supported by the Portuguese Foundation for Science and Technology (FCT) under Project PTDC/EEI-TEL/1448/2012.

The authors are with the Instituto de Telecomunicações, Instituto Superior Técnico, Technical University of Lisbon, 1049-001 Lisbon, Portugal (e-mail: brandao.faria@ieee.org; miguel.p.pires@googlemail.com).

Digital Object Identifier 10.1109/TMTT.2012.2210439

II. Problem Formulation

Transmission lines (ELTLs and MGTLs) support a multitude of propagation modes depending on its geometry and operating frequency. However, only the lowest order mode will be examined—the fundamental TEM mode, which, strictly speaking, only applies to lossless transmisson lines. Nonetheless, the perturbations arising from wires' imperfection and dielectric imperfection will be taken into account. Therefore, the theory developed in the paper fits in a quasi-TEM framework. In addition, the wires and the dielectric medium are assumed to be characterized by linear constitutive parameters.

A. ELTL

Here, the standard two-wire ELTL theory is briefly described. Consider a uniform homogeneous ELTL made of two parallel conductors of length l, fed by a sinusoidal electromotive force (EMF), and terminated on a linear load [see Fig. 1(a)]. Note that the longitudinal z-axis is oriented from right to left.

The electric wires are characterized by conductivity σ_E, permittivity ε_E, and permeability μ_E. On the other hand, the dielectric medium is characterized by permeability μ_0, and complex permittivity $\bar{\varepsilon} = \varepsilon' - j\varepsilon'' = \varepsilon(1 - j\delta)$, where the loss tangent δ includes both polarization and conduction dielectric losses.

In an ELTL, the consideration of conductors' imperfection $(\sigma_E \neq \infty)$ gives rise to a weak longitudinal component E_z of the electric field, which is responsible for the change of field character from TEM to quasi-TEM.

The flow of energy from the generator to the load is locally determined by the flux of the Poynting vector across the transverse plane surface $S_{\mathrm{Trans}}(z = \text{constant})$, [1], [4], [5]

$$p(z,t) = \int\limits_{S_{\mathrm{Trans}}} (\mathbf{E} \times \mathbf{H}) \bullet (-\vec{e}_z) dS = i(z,t) v(z,t). \quad (1)$$

According to standard frequency-domain ELTL theory, $(e^{j\omega t})$, the complex amplitudes of the line voltage and line current obey the propagation equations, [5], [6]

$$\begin{cases} \dfrac{d}{dz}\overline{V}(z) = \overbrace{\left(\overline{Z}_{\mathrm{skin}}(\omega) + j\omega L\right)}^{\overline{Z}_E}\overline{I}(z) \\ \dfrac{d}{dz}\overline{I}(z) = \underbrace{(j\omega\overline{C})}_{\overline{Y}_E}\overline{V}(z) = \underbrace{(G + j\omega C)}_{\overline{Y}_E}\overline{V}(z) \end{cases} \quad (2)$$

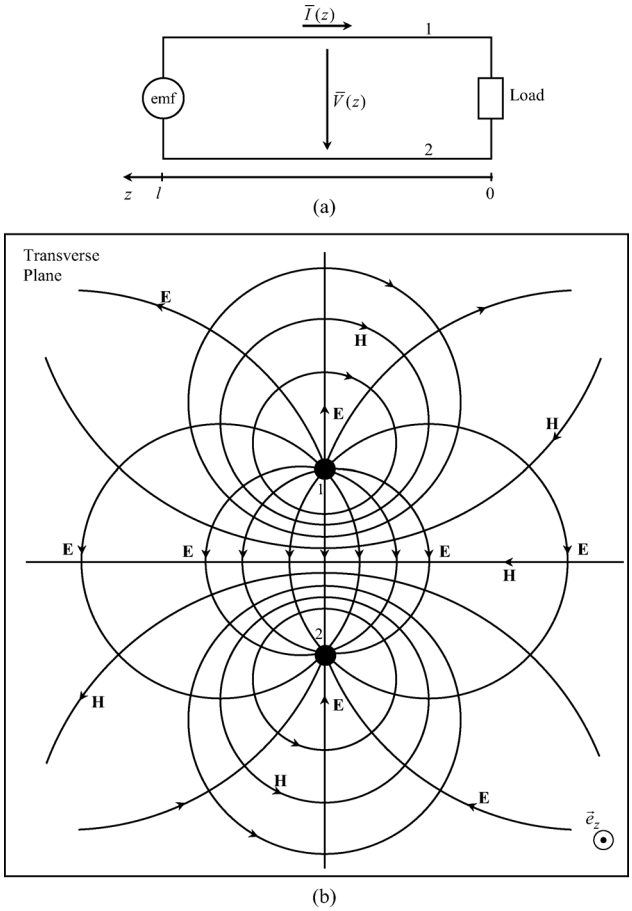

Fig. 1. (a) ELTL driven by EMF. (b) Transverse plane cross-sectional view showing TEM fields (example of a symmetric bifilar line with perfect electric wires).

where L, $\overline{C}$, and $\overline{Z}_{\rm skin}$, respectively, denote the external inductance, complex capacitance, and skin-effect impedance, per unit length (pul) of the line. We also have $C = \mathrm{Re}(\overline{C})$ and $G = \omega C\delta$.

The L and $\overline{C}$ line parameters depend on the line geometry and on the dielectric medium properties, [5], [6]

$$L = g_E\mu_0; \overline{C} = \overline{\varepsilon}/g_E = C(1 - j\delta) \tag{3}$$

where g_E is a dimensionless geometrical parameter; e.g., planar line (width w, separation s): $g_E = s/w$; coaxial geometry (radii r_1 and r_2): $g_E = (1/2\pi)\ln(r_2/r_1)$; bifilar line (radius r, separation s): $g_E = (1/\pi)\mathrm{acosh}(s/2r)$.

The solution of (2) is also well known [5], [6]

$$\begin{cases} \overline{V}(z) = \overline{V}_i e^{\overline{\gamma}z} \times (1 + \overline{\Gamma} e^{-2\overline{\gamma}z}) \\ \overline{I}(z) = \dfrac{\overline{V}_i}{\overline{Z}_w^E} e^{\overline{\gamma}z} \times (1 - \overline{\Gamma} e^{-2\overline{\gamma}z}) \end{cases} \tag{4}$$

where

$\overline{V}_i$ complex amplitude of the incident wave voltage at the load terminals;

$\overline{\gamma} = \sqrt{\overline{Z}_E \overline{Y}_E}$ propagation constant;

$\overline{\Gamma} = (\overline{Z}_0^E - \overline{Z}_w^E)/(\overline{Z}_0^E + \overline{Z}_w^E)$ load reflection factor;

$\overline{Z}_w^E = \sqrt{\overline{Z}_E/\overline{Y}_E}$ characteristic impedance of the line.

$\overline{Z}_0^E$ load impedance.

Considering an ELTL section of axial length l, the input and output voltages and currents are related by means of a transmission matrix $\overline{T}_E$ given by [5], [6]

$$\begin{bmatrix} \overline{V} \\ \overline{I} \end{bmatrix}_{\rm in} = \underbrace{\begin{bmatrix} \cosh(\overline{\gamma}l) & \sinh(\overline{\gamma}l)\overline{Z}_w^E \\ (\overline{Z}_w^E)^{-1}\sinh(\overline{\gamma}l) & \cosh(\overline{\gamma}l) \end{bmatrix}}_{\overline{T}_E} \begin{bmatrix} \overline{V} \\ \overline{I} \end{bmatrix}_{\rm out}. \tag{5}$$

B. MGTL

We wish to introduce, discuss, and analyze the concept of an MGTL, which is to be viewed as the dual version of an ELTL, where the roles played by **E** and **H** are interchanged.

The MGTL is a closed magnetic circuit fed by a sinusoidal magnetomotive force (MMF) and terminated on a linear load (see Fig. 2). The magnetic wires are characterized by conductivity σ_M, permittivity ε_M, and permeability μ_M. The dielectric medium is characterized by permeability μ_0, and complex permittivity $\overline{\varepsilon} = \varepsilon' - j\varepsilon'' = \varepsilon(1 - j\delta)$, where the loss tangent δ includes both polarization and conduction dielectric losses. Details concerning the driving MMF and the load will be addressed in Section V.

In an MGTL, the consideration of wires' imperfection ($\mu_M \neq \infty$) gives rise to a weak longitudinal component H_z of the magnetic field, which is responsible for the change of field character from TEM to quasi-TEM.

The duality between ELTLs and MGTLs is a result of the equivalence among the integral variables shown in (6) and (7). Note, however that, complete duality does not exist at a physical level. In fact, there is an asymmetry resulting from the fact that the electric current intensity is the result of electron motion, while the magnetic flux is not the result of magnetic monopole motion (magnetic monopoles do not exist)

$$\begin{cases} \text{Current intensity [A]} \\ i(z,t) = \displaystyle\int_{S_e} \mathbf{J} \bullet \vec{n}\, dS \end{cases} \leftrightarrow \begin{cases} \text{Magnetic flux time derivative [V]} \\ \varphi(z,t) = \dfrac{\partial}{\partial t}\phi(z,t) = \displaystyle\int_{S_m} \frac{\partial \mathbf{B}}{\partial t} \bullet \vec{n}\, dS \end{cases} \tag{6}$$

$$\begin{cases} \text{Electric voltage [V]} \\ v(z,t) = \displaystyle\int_{\vec{12}} \mathbf{E} \bullet d\vec{s} \end{cases} \leftrightarrow \begin{cases} \text{Magnetic voltage [A]} \\ u(z,t) = \displaystyle\int_{\vec{12}} \mathbf{H} \bullet d\vec{s} \end{cases}. \tag{7}$$

In (6), S_e denotes the cross-sectional area of the electric wires of the ELTL. Likewise, S_m denotes the cross-sectional area of the magnetic wires of the MGTL. Also in (6), the unit vector $\vec{n}$ normal to S_e and to S_m denotes the reference direction assigned to i and ϕ. In (7), the line integrals between wires 1 and 2 are evaluated in the transverse plane (z = constant).

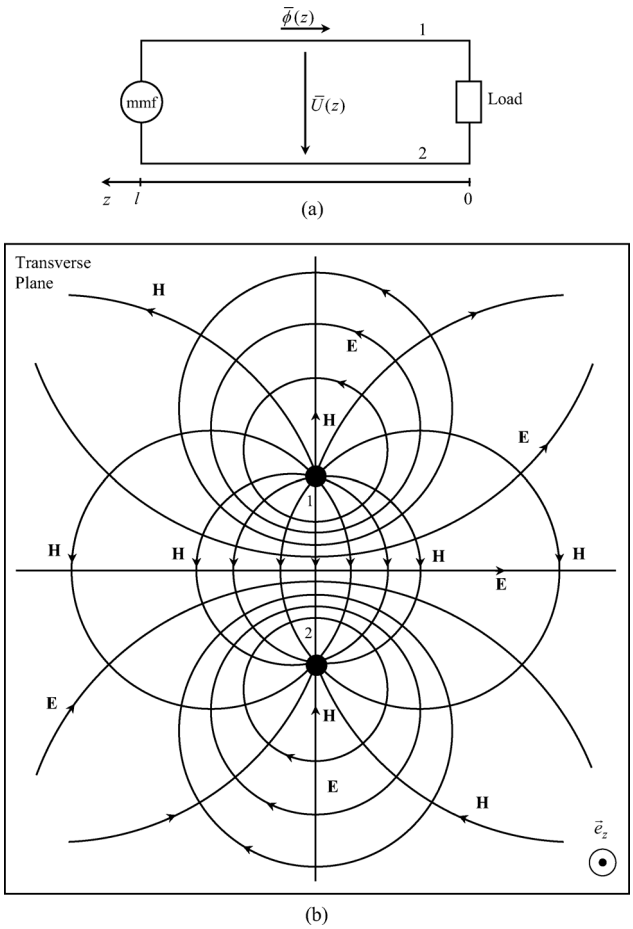

Fig. 2. (a) MGTL driven by MMF. (b) Transverse plane cross-sectional view of the MGTL showing TEM fields (example of a symmetric bifilar line with perfect magnetic wires).

The flow of energy from the generator to the load is locally determined by the flux of the Poynting vector across the transverse plane surface $S_{\rm Trans}(z = \text{constant})$ [1]

$$p(z,t) = \int\limits_{S_{\rm Trans}} (\mathbf{E} \times \mathbf{H}) \bullet (-\vec{e}_z) dS = u(z,t)\varphi(z,t). \quad (8)$$

While in (6), $\mathbf{J}$ and $\mathbf{B}$ are axial directed vectors, $\mathbf{E}$ and $\mathbf{H}$ in (7) are, dominantly transverse vectors, $\perp \vec{e}_z$.

In an ELTL, the transverse $\mathbf{E}$ field is related to capacitive effects between electric wires originated by electric charges. However, in an MGTL, the transverse $\mathbf{H}$ field is related to transverse magnetic leakage between magnetic wires.

Note that magnetic leakage does occur even if the magnetic wires have $\mu_M \to \infty$. To clarify this aspect we do not need to consider the added complication arising from time-varying fields. In fact, by applying Ampère law to the magnetic circuit in Fig. 3, we obtain

$$\oint\limits_{\overrightarrow{aba}} \mathbf{H} \bullet d\vec{s} = \int\limits_{ab} \mathbf{H}_{\rm air} \bullet d\vec{s} + \int\limits_{ba} \mathbf{H}_{\rm Fe} \bullet d\vec{s} = \int\limits_{S} \mathbf{J} \bullet \vec{n}_S dS = NI. \quad (9)$$

The integration surface S, in (9), is the rectangular plane corresponding to the closed path aba, and $\vec{n}_S$ is the associated

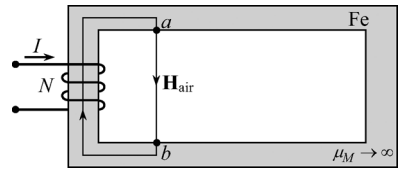

Fig. 3. Magnetic leakage between two perfect magnetic wires.

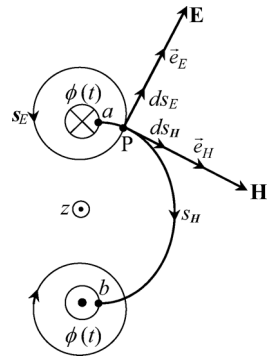

Fig. 4. Application of Faraday's law to a closed path s_E coinciding with a field line of $\mathbf{E}$. A leakage field line of $\mathbf{H}$ is also displayed.

Stoke's normal. Since $\mathbf{H}_{\rm Fe} = 0$ inside the perfect magnetic wires (path ba), the magnetic voltage U_{ab} corresponding to $\mathbf{H}_{\rm air}$ cannot be zero, $U_{ab} = NI$, and therefore, $\mathbf{H}_{\rm air} \neq 0$.

Another distinguishing feature that must be brought to attention is that, in an homogeneous ELTL, the transverse $\mathbf{E}$ field is a gradient field, $\mathbf{E} = -\nabla\Phi_E$, whose field lines are open, starting and ending at the electric wires. The transverse $\mathbf{H}$ field is a solenoidal field, $\nabla \bullet \mathbf{H} = 0$, whose field lines are closed, encircling the electric wires.

Conversely, in a homogeneous MGTL, the transverse $\mathbf{E}$ field is a solenoidal induction field, $\nabla \bullet \mathbf{E} = 0$, whose field lines are closed, encircling the magnetic wires. The transverse $\mathbf{H}$ field is a gradient field, $\mathbf{H} = -\nabla\Phi_M$, whose field lines are open, starting and ending at the magnetic wires.

III. MGTL Propagation Equations

The transverse electric induction field $\mathbf{E}_k(z,t)$, associated to the time-varying magnetic flux carried by the two magnetic wires, is related to the magnetic flux $\phi(z,t)$ itself, through the frequency-domain Faraday law (Fig. 4)

$$\oint\limits_{\vec{s}_E} \overline{E}\vec{e}_E \bullet d\vec{s} = \oint\limits_{\vec{s}_E} \overline{E} ds_E = -j\omega \int\limits_{S_m} \overline{\mathbf{B}} \bullet \vec{e}_z dS = +j\omega\overline{\phi} = \overline{\varphi} \quad (10)$$

where ds_E is an infinitesimal path length belonging to a transverse closed field line of $\mathbf{E}$ embracing the magnetic wire #1; the field direction being defined by the unit vector $\vec{e}_E$.

At a given point $P(x,y)$ belonging to the transverse plane, the scalar complex amplitude $\overline{E}$ is proportional to the magnetic flux time rate

$$\overline{E} = \frac{\overline{\varphi}(z)}{\xi_E(x,y)}. \quad (11)$$

The direction of $\vec{e}_E$, as well as the function ξ_E (units: m), depend on the observation point P and on the particular geometry of the MGTL.

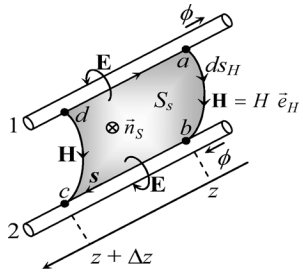

Fig. 5. Application of Ampère's generalized law to the path s.

A. Equation for $d\overline{U}/dz$

Let us pay attention to the longitudinal variation of the magnetic voltage along the line.

Let $\overline{U}(z)$ and $\overline{U}(z+\Delta z)$ represent the complex amplitudes of the transverse magnetic voltages referred to the z and $z+\Delta z$ transverse planes, respectively, where the length Δz is vanishingly small.

Next, consider the application of the generalized Ampère law, [5], to the path $\vec{s} = abcda$ shown in Fig. 5

$$\oint_{\vec{s}} \overline{\mathbf{H}} \bullet d\vec{s} = j\omega\overline{\varepsilon} \int_{S_s} \overline{\mathbf{E}} \bullet \vec{n}_S \, dS. \tag{12}$$

The subpaths bc and da of length Δz are longitudinal. The subpaths ab and cd are chosen coincident with $\mathbf{H}$-field transverse lines. Therefore, the Stokes's unit normal $\vec{n}_S$ to the surface S_s is antiparallel to the transverse $\mathbf{E}$ field crossing S_s.

Evaluation of the line and surface integrals in (12) yields

$$\oint_{\vec{s}} \overline{\mathbf{H}} \bullet d\vec{s} = \overline{U}(z) + \overline{U}_2 \Delta z - \overline{U}(z+\Delta z) + \overline{U}_1 \Delta z \tag{13a}$$

$$\int_{S_s} \overline{\mathbf{E}} \bullet \vec{n}_S \, dS = \overline{\psi}_E = -\int_{S_s} \overline{E} \, dS = -\int_{S_s} \overline{E} \, \Delta z \, ds_H \tag{13b}$$

where ds_H is an infinitesimal path length belonging to a transverse open field line of $\mathbf{H}$.

The terms $\overline{U}_1$ and $\overline{U}_2$ in (13a) represent the pul magnetic voltage drops associated to the weak component H_z arising from the fact that the magnetic wires are not magnetically perfect, $\mu_M \neq \infty$. Both terms are proportional to the magnetic flux $\overline{\phi}(z)$ carried by the magnetic wires. We can then write

$$\overline{U}_1 + \overline{U}_2 = \overline{R} m_{\text{skin}} \overline{\phi}(z) \leftrightarrow j\omega(\overline{U}_1 + \overline{U}_2) = \overline{R} m_{\text{skin}} \overline{\varphi}(z) \tag{14}$$

where $\overline{R} m_{\text{skin}}$ is the pul skin-effect complex magnetic reluctance of the MGTL. This parameter, which depends on the frequency, can be evaluated using skin-effect theory (see Appendix A).

The quantity $\overline{\psi}_E$ in (13b) denotes the electric induction flux across the open surface S_s shown in Fig. 5. Taking (11) and (13b) into account, we can write

$$\overline{\psi}_E = -\Delta z \underbrace{\int_{S_s} \frac{ds_H}{\xi_E(x,y)}}_{g_M} \overline{\varphi}(z) = -(g_M \Delta z)\overline{\varphi}(z) \tag{15}$$

where g_M is a positive dimensionless geometrical factor that only depends on the particular geometry of the MGTL.

At last, plugging (14) and (15) into (13), dividing both sides of the resulting equation by Δz and taking the limit $\Delta z \to 0$, we find the relationship between the z-variation of the magnetic voltage along the MGTL and the magnetic flux flowing in the magnetic wires

$$\frac{d}{dz}\overline{U}(z) = \overbrace{\left(\frac{\overline{R} m_{\text{skin}}}{j\omega} + j\omega\overline{\varepsilon} g_M\right)}^{\overline{Y}_M} \overline{\varphi}(z). \tag{16}$$

The frequency-dependent parameter $\overline{Y}_M$ has the physical dimensions of a pul admittance (in siemens/meter).

The imaginary and real parts of the first term in the right-hand side of (16) are associated, respectively, to magnetic wire losses, and to electric and magnetic energy storage inside the magnetic wires. The second term $j\omega\overline{\varepsilon} g_M$ is related to electric energy storage and power losses in the dielectric medium. Magnetic energy storage in the dielectric medium is accounted in (25) through $j\omega\mu_0/g_M$.

B. Equation for $d\overline{\phi}/dz$

Now let us pay attention to the longitudinal variation of the magnetic flux along the line. Let $\overline{\phi}(z)$ and $\overline{\phi}(z+\Delta z)$ represent the complex amplitudes of the axial magnetic fluxes referred to the z and $z+\Delta z$ transverse planes, respectively, where the length Δz is vanishingly small.

In an MGTL, the transverse $\mathbf{H}$ field is a gradient field whose lines of force are open, starting and ending at the magnetic wires of the line (see Fig. 4). In the transverse plane (z = constant), the line integral of $\mathbf{H}$ from wire 1 to wire 2 yields the magnetic voltage

$$\overline{U}(z) = \int_{\vec{12}} \overline{H} \vec{e}_H \bullet d\vec{s} = \int_{\vec{12}} \overline{H} ds_H. \tag{17}$$

Therefore, at a given point $P(x,y)$ on the transverse plane, we can write

$$\overline{H} = \frac{\overline{U}(z)}{\xi_H(x,y)}. \tag{18}$$

The direction of $\vec{e}_H$, as well as the function ξ_H (unit: m), depend on the observation point P and on the particular geometry of the MGTL.

Next, consider the application of $\nabla \bullet \overline{\mathbf{B}} = 0$ in its integral form

$$\int_{S_V} \overline{\mathbf{B}} \bullet \vec{n}_o \, dS = 0 \tag{19}$$

where S_V is a closed surface of axial length Δz that encircles the magnetic wire 1, and $\vec{n}_o$ is the outward unit normal (see Fig. 6).

The shape of the lateral surface S_{lat} belonging to S_V is purely arbitrary because $\mathbf{B}$ is a purely solenoidal field. Therefore, we

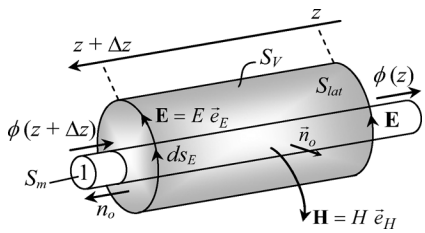

Fig. 6. Application of $\nabla \bullet \mathbf{B} = 0$ to a closed surface S_V enclosing the flux-carrying magnetic wire #1.

can choose $S_{\rm lat}$ in a way such that it orthogonally intersects the open surface S_s considered in the evaluation of $\overline{\psi}_E$ in (15)

$$\int_{S_V} \overline{\mathbf{B}} \bullet \vec{n}_o dS = 0$$

$$= \underbrace{\int_{S_m(z)} \overline{\mathbf{B}} \bullet (-\vec{e}_z) dS}_{\overline{\phi}(z)} + \underbrace{\int_{S_m(z+\Delta z)} \overline{\mathbf{B}} \bullet \vec{e}_z dS}_{-\overline{\phi}(z+\Delta z)} + \underbrace{\int_{S_{\rm lat}} \overline{\mathbf{B}} \bullet \vec{n}_o dS_{\rm lat}}_{\overline{\phi}_{\rm leakage}}. \quad (20)$$

As a parenthetical remark, it may be noticed that the result in (20) is similar to Kirchhoff's current law, $\sum_{\rm node} \overline{I} = 0$, valid for quasi-stationary regimes, where $\nabla \bullet \overline{\mathbf{J}} \approx 0$ [5].

In (20), the leakage flux corresponds to field lines of $\mathbf{B} = \mu_0 \mathbf{H}$ that cross the lateral surface $S_{\rm lat}$. Taking (17) into account, and noting that $\vec{n}_o = \vec{e}_H$ and $dS_{\rm lat} = \Delta z ds_E$, we can write

$$\overline{\phi}_{\rm leakage} = \mu_0 \int_{S_{\rm lat}} \overline{H}\, dS_l = \mu_0 \Delta z \underbrace{\int_{S_{\rm lat}} \frac{ds_E}{\xi_H(x,y)}}_{g'_M} \overline{U}(z) \quad (21a)$$

or

$$\overline{\phi}_{\rm leakage} = g'_M \mu_0 \Delta z \overline{U}(z) = \mu_0 \frac{\Delta z}{g_M} \overline{U}(z). \quad (21b)$$

The identity

$$g'_M = 1/g_M \quad (22)$$

is a result of the relationship between electric and magnetic field values in the transverse plane. (This assertion is analyzed in Appendix B).

From (20) and (21), we get

$$\overline{\phi}(z + \Delta z) - \overline{\phi}(z) = \frac{\mu_0}{g_M} \Delta z \overline{U}(z). \quad (23)$$

At last, considering (23), dividing both sides of the equation by Δz, and taking the limit $\Delta z \to 0$, we find the relationship between the z-variation of the magnetic flux along the MGTL and the magnetic voltage between the two magnetic wires

$$\frac{d}{dz} \overline{\phi}(z) = \left(\frac{\mu_0}{g_M} \right) \overline{U}(z) \quad (24)$$

or, taking into account that $\overline{\varphi} = j\omega \overline{\phi}$,

$$\frac{d}{dz} \overline{\varphi}(z) = \overbrace{\left(\frac{j\omega\mu_0}{g_M} \right)}^{\overline{Z}_M} \overline{U}(z). \quad (25)$$

The frequency-dependent parameter $\overline{Z}_M$ has physical dimensions of a pul impedance [Ω/m].

From (16) and (25), the frequency-domain domain equations for an MGTL can be summarized as shown in (26), where the similitude with (2) is evident

$$\begin{cases} \dfrac{d}{dz} \overline{U}(z) = \overline{Y}_M \overline{\varphi}(z) \\ \dfrac{d}{dz} \overline{\varphi}(z) = \overline{Z}_M \overline{U}(z). \end{cases} \quad (26)$$

C. Lossless MGTL—Time Domain

For the lossless line case, $\mu_M \to \infty, \overline{\varepsilon} \to \varepsilon + j0$, (26) yields

$$\begin{cases} \dfrac{d}{dz} \overline{U}(z) = j\omega\varepsilon g_M \overline{\varphi}(z) \\ \dfrac{d}{dz} \overline{\varphi}(z) = \dfrac{j\omega\mu_0}{g_M} \overline{U}(z). \end{cases} \quad (27)$$

Taking into account that for time–harmonic regimes, $\partial/\partial t \leftrightarrow j\omega$, the time-domain propagation equations, corresponding to (27), translate to

$$\begin{cases} \dfrac{\partial}{\partial z} u(z,t) = \varepsilon g_M \dfrac{\partial}{\partial t} \varphi(z,t) \\ \dfrac{\partial}{\partial z} \varphi(z,t) = \dfrac{\mu_0}{g_M} \dfrac{\partial}{\partial t} u(z,t). \end{cases} \quad (28)$$

From the above results, we can readily obtain

$$\frac{\partial^2}{\partial z^2} \begin{Bmatrix} u(z,t) \\ \varphi(z,t) \end{Bmatrix} = \mu_0 \varepsilon \frac{\partial^2}{\partial t^2} \begin{Bmatrix} u(z,t) \\ \varphi(z,t) \end{Bmatrix} \quad (29)$$

showing that both u and φ do satisfy the same wave equation, the wave propagation velocity being given by $v_w = 1/\sqrt{\mu_0 \varepsilon}$. It must be remarked that the expected result in (29) would not be obtained if the identity (22) were false. Moreover, for MGTLs and ELTLs of identical geometry, the geometrical factors g_M and g_E are also identical

$$g_E = g_M = g. \quad (30)$$

IV. Frequency-Domain Solution of the Propagation Equations for Lossy MGTLs

Using (3), (30), (16), and (25), the pair of equations in (26) can be rewritten as

$$\begin{cases} \dfrac{d}{dz} \overline{U}(z) = \overbrace{(j\omega \overline{C} g^2 + \Delta \overline{Y}_M)}^{\overline{Y}_M} \overline{\varphi}(z) \\ \dfrac{d}{dz} \overline{\varphi}(z) = \underbrace{\left(\dfrac{j\omega L}{g^2} \right)}_{\overline{Z}_M} \overline{U}(z) \end{cases} \quad (31)$$

where L and $\overline{C}$ are the familiar pul external inductance and pul complex capacitance of an ELTL with the same geometry. The perturbation term $\Delta\overline{Y}_M$

$$\Delta\overline{Y}_M = \frac{\overline{R}m_{\rm skin}}{j\omega} \tag{32}$$

is associated to MGTL wire losses and wire internal energy storage (skin effect).

It is interesting to note that, in the case of the ELTL, contributions from losses appear in the two equations of (2), whereas in the MGTL, all the losses are included in the top equation of (31). A possible interpretation for this apparent asymmetry is the already referred nonexistence of magnetic monopoles. This asymmetry, i.e., the absence of a real part in $\overline{Z}_M$, also leads to the conclusion that a distortionless condition for MGTLs cannot be established.

From (31), we obtain

$$\begin{cases} \dfrac{d^2}{dz^2}\overline{\varphi}(z) - \overline{Z}_M\overline{Y}_M\overline{\varphi}(z) = 0 \\ \overline{U}(z) = \dfrac{1}{\overline{Z}_M}\dfrac{d}{dz}\overline{\varphi}(z). \end{cases} \tag{33}$$

The top equation in (33) is a homogeneous second-order differential equation with constant coefficients. Its solution is trivial

$$\overline{\varphi}(z) = \overline{\varphi}_i e^{\overline{\gamma}z} + \overline{\varphi}_r e^{-\overline{\gamma}z} \tag{34}$$

where $\overline{\gamma}$, the propagation constant, is given by

$$\overline{\gamma} = \sqrt{\overline{Z}_M\overline{Y}_M}. \tag{35}$$

The constants $\overline{\varphi}_i$ and $\overline{\varphi}_r$ are the complex amplitudes of the incident and reflected magnetic flux rate waves at $z = 0$. These constants are obtained upon consideration of the MGTL boundary conditions. The load boundary condition $(z = 0)$ will allow $\overline{\varphi}_i$ and $\overline{\varphi}_r$ to be related through the load reflection factor $\overline{\Gamma}$

$$\overline{\Gamma} = \frac{\overline{\varphi}_r}{\overline{\varphi}_i} = \frac{\overline{\phi}_r}{\overline{\phi}_i}. \tag{36}$$

By making use of (36), we can rewrite (34) as

$$\overline{\varphi}(z) = \overline{\varphi}_i e^{\overline{\gamma}z} \times (1 + \overline{\Gamma}e^{-2\overline{\gamma}z}). \tag{37}$$

The bottom equation in (33) allows for the determination of the magnetic voltage solution

$$\overline{U}(z) = \frac{\overline{\varphi}_i}{\overline{Z}_w^M} e^{\overline{\gamma}z} \times (1 - \overline{\Gamma}e^{-2\overline{\gamma}z}) \tag{38}$$

where $\overline{Z}_w^M$ is the magnetic characteristic wave impedance (Ω) of the line

$$\overline{Z}_w^M = \sqrt{\frac{\overline{Z}_M}{\overline{Y}_M}} \tag{39}$$

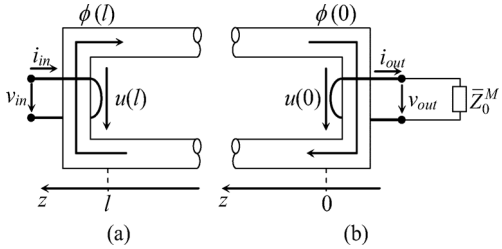

Fig. 7. MGTL terminations. (a) Sending end. (b) Receiving end.

note that, in the case of a lossless MGTL, we would find

$$\left(Z_w^M\right)_{\rm lossless} = \frac{1}{g^2}\sqrt{\frac{L}{C}} = \frac{1}{g}\sqrt{\frac{\mu_0}{\varepsilon}}. \tag{40}$$

Dividing (37) by (38), considering $z = 0$, we obtain the magnetic load impedance

$$\frac{\overline{\varphi}(0)}{\overline{U}(0)} = \overline{Z}_0^M = \overline{Z}_w^M\frac{1+\overline{\Gamma}}{1-\overline{\Gamma}} \tag{41}$$

from where the load reflection factor $\overline{\Gamma}$ can be evaluated

$$\overline{\Gamma} = \frac{\overline{Z}_0^M - \overline{Z}_w^M}{\overline{Z}_0^M + \overline{Z}_w^M}. \tag{42}$$

Likewise, dividing (37) by (38), considering $z = l$, we obtain the magnetic input impedance of the line

$$\frac{\overline{\varphi}(l)}{\overline{U}(l)} = \overline{Z}_l^M = \overline{Z}_w^M\frac{1+\overline{\Gamma}e^{-2\overline{\gamma}l}}{1-\overline{\Gamma}e^{-2\overline{\gamma}l}}. \tag{43}$$

The complex amplitude of the incident wave $\overline{\varphi}_i$ can be determined from (37) or (38) once one of the following quantities, $\overline{\phi}(0)$, $\overline{\phi}(l)$, $\overline{U}(0)$ or $\overline{U}(l)$, is specified.

V. Sending and Receiving Ends of an MGTL

Here we analyze how the energy guided by the MGTL can be injected into to the line (at $z = l$), and afterwards, delivered to a load (at $z = 0$).

The line excitation can be provided by a current-carrying loop embracing the vertical magnetic piece placed at $z = l$ [see Fig. 7(a)].

The MMF source shown in Fig. 2 is to be identified with the current $\overline{I}_{\rm in}$ in the excitation loop. Therefore, the magnetic voltage at $z = l$ is given by

$$\overline{U}(l) = \overline{I}_{\rm in}. \tag{44}$$

The electric voltage $\overline{V}_{\rm in}$ applied to the excitation loop determines the magnetic flux at $z = l$

$$j\omega\overline{\phi}(l) = \overline{\varphi}(l) = \overline{V}_{\rm in}. \tag{45}$$

The coupling of the MGTL to an external impedance load can be provided by another conducting loop embracing the vertical magnetic piece placed at $z = 0$ [see Fig. 7(b)].

The magnetic flux $\overline{\phi}(0)$ is converted into a load voltage through

$$\overline{V}_{\rm out} = j\omega\overline{\phi}(0) = \overline{\varphi}(0) \tag{46}$$

whereas the magnetic voltage $\overline{U}(0)$ is converted into a load current through

$$\overline{I}_{\rm out} = \overline{U}(0). \tag{47}$$

The load impedance of the MGTL is

$$\frac{\overline{V}_{\rm out}}{\overline{I}_{\rm out}} = \frac{\overline{\varphi}(0)}{\overline{U}(0)} = \overline{Z}_0^M \tag{48}$$

from where, according to (42), the load reflection factor $\overline{\Gamma}$ can be evaluated.

The situation $\overline{\Gamma} = 0$—matched line ($\overline{\phi}_r = 0$)—is achieved when

$$\overline{Z}_0^M = \overline{Z}_w^M. \tag{49}$$

For a lossless MGTL, the matched line condition in (49) turns into $\overline{Z}_0^M = \sqrt{L/C}$.

If the receiving end conducting loop is open ($\overline{I}_{\rm out} = 0$), then $\overline{Z}_0^M = \infty$. As a result, we have $\overline{\Gamma} = 1$ and $\overline{U}(0) = 0$ (a magnetic short-circuit termination).

At this point, we can easily establish the transmission matrix of an MGTL section of axial length l taking into account its external coupling devices

$$\begin{bmatrix}\overline{V}\\ \overline{I}\end{bmatrix}_{\rm in} = \overline{T}_M \begin{bmatrix}\overline{V}\\ \overline{I}\end{bmatrix}_{\rm out}. \tag{50}$$

By particularizing the results in (37) and (38), for $z = 0$ and $z = l$, and making use of (44)–(47), we obtain, similarly to (5),

$$\overline{T}_M = \begin{bmatrix} \cosh(\overline{\gamma}l) & \sinh(\overline{\gamma}l)\overline{Z}_w^M \\ \left(\overline{Z}_w^M\right)^{-1}\sinh(\overline{\gamma}l) & \cosh(\overline{\gamma}l)\end{bmatrix}. \tag{51}$$

VI. Wave Parameters Approximate Calculation

For a better understanding of the results in Sections IV and V, it would help to find approximate results for the wave parameters of the MGTL, i.e., the propagation constant $\overline{\gamma}$ in (35), and the magnetic characteristic wave impedance $\overline{Z}_w^M$ in (39) for the case of small losses. This step will shed some light on the role played by the perturbations arising from the different loss mechanisms as far as the evaluation of the wave parameters is concerned.

Assuming that $|\Delta\overline{Y}_M|g^2 \ll \omega|\overline{C}|$, the propagation constant in (35) and the characteristic impedance in (39) can be simplified. By making use of (32), one gets

$$\overline{\gamma} = \sqrt{\overline{Z}_M.\overline{Y}_M} = \alpha + \frac{j\omega}{v_p} \approx \frac{j\omega}{v_w}\left(1 - \frac{\overline{R}m_{\rm skin}}{2\omega^2\varepsilon g} - j\frac{\delta}{2}\right) \tag{52}$$

$$\overline{Z}_w^M = \sqrt{\frac{\overline{Z}_M}{\overline{Y}_M}} \approx \frac{1}{g}\sqrt{\frac{\mu_0}{\varepsilon}}\left(1 + \frac{\overline{R}m_{\rm skin}}{2\omega^2\varepsilon g} + j\frac{\delta}{2}\right) \tag{53}$$

TABLE I
Wave Parameters of MGTL and ELTL

	MGTL	ELTL
α	$\frac{\omega}{2v_w}\left(\delta + \frac{X_M}{\omega^2\varepsilon g}\right)$	$\frac{\omega}{2v_w}\left(\delta + \frac{R_E}{\omega\mu_0 g}\right)$
$\frac{v_p}{v_w}$	$\left(1 + \frac{R_M}{2\omega^2\varepsilon g}\right)$	$\left(1 - \frac{X_E}{2\omega\mu_0 g}\right)$
$\frac{R_w}{R_D}$	$\frac{1}{g}\left(1 + \frac{R_M}{2\omega^2\varepsilon g}\right)$	$g\left(1 + \frac{X_E}{2\omega\mu_0 g}\right)$
$\frac{X_w}{R_D}$	$\frac{1}{2g}\left(\delta + \frac{X_M}{\omega^2\varepsilon g}\right)$	$\frac{g}{2}\left(\delta - \frac{R_E}{\omega\mu_0 g}\right)$

and from (52), it follows:

$$\alpha \approx \frac{\omega}{2v_w}\left(\delta + \frac{{\rm Im}(\overline{R}m_{\rm skin})}{\omega^2\varepsilon g}\right) \tag{54a}$$

$$v_p \approx v_w\left(1 + \frac{{\rm Re}(\overline{R}m_{\rm skin})}{2\omega^2\varepsilon g}\right) \tag{54b}$$

where α and v_p denote the attenuation constant and phase velocity. With regard to the characteristic impedance, we find from (53)

$${\rm Re}\left(\overline{Z}_w^M\right) \approx \frac{1}{g}\sqrt{\frac{\mu_0}{\varepsilon}}\left(1 + \frac{{\rm Re}(\overline{R}m_{\rm skin})}{2\omega^2\varepsilon g}\right) \tag{55a}$$

$${\rm Im}\left(\overline{Z}_w^M\right) \approx \frac{1}{2g}\sqrt{\frac{\mu_0}{\varepsilon}}\left(\delta + \frac{{\rm Im}(\overline{R}m_{\rm skin})}{\omega^2\varepsilon g}\right). \tag{55b}$$

Comparison established between (54) and (55) allows the following conclusion:

$$\begin{cases} \dfrac{v_p}{v_w} = \dfrac{{\rm Re}\left(\overline{Z}_w^M\right)}{(Z_w^M)_{\rm lossless}} \\ \dfrac{\alpha v_w}{\omega} = \dfrac{{\rm Im}\left(\overline{Z}_w^M\right)}{(Z_w^M)_{\rm lossless}}. \end{cases} \tag{56}$$

Table I compares the above results with those resulting from a similar analysis of the ELTL. For the sake of brevity, the following compact notation is used:

$$\begin{cases} {\rm Re}\left(\overline{Z}_{\rm skin}(\omega)\right) = R_E \\ {\rm Im}\left(\overline{Z}_{\rm skin}(\omega)\right) = X_E \end{cases}, \begin{cases} {\rm Re}\left(\overline{R}m_{\rm skin}(\omega)\right) = R_M \\ {\rm Im}\left(\overline{R}m_{\rm skin}(\omega)\right) = X_M \end{cases} \tag{57}$$

and $R_D = \sqrt{\mu_0/\varepsilon}$.

VII. Discussion

The theory presented through Sections II–VI is clear and sound. However, the fabrication, technology, and applications of MGTLs are uncharted territory. The impact of MGTLs in electrical engineering is, at this point, speculative matter. Only the future will tell about MGTL developments.

A look at Table I suggests that MGTLs may possibly have an advantage over ELTLs at high-frequency regimes because of the way through which the skin-effect terms intervene in the calculation of the propagation parameters. While in the ELTL case, the skin-effect perturbations appear divided by ω, in the MGTL case, they appear divided by ω^2. For high-frequency ELTLs,

the skin-effect term increases with $\omega^{1/2}$. From Table I, we see that MGTLs may offer comparative advantages if the skin-effect term varies proportionally to ω^p with $p < (3/2)$. Consequently, we verify that the key issue with MGTLs is the frequency behavior of the material medium of which the magnetic wires will be made of.

For high-frequency magnetic-systems applications, ferrites are the most usual material. Ferrites have been used with great success in microwave devices [13], as for example, circulators, isolators, phase shifters, and filters. In those applications, ferrites are traversed by electromagnetic waves, but in the case of MGTLs, they will be used as magnetic wires to carry a magnetic flux; the electromagnetic field, guided by the magnetic wires, travels through a dielectric medium. Therefore, the circumstances are not the same.

Soft ferrites are very poorly conductive materials, and as such, they combine the properties of a magnetic medium with that of an electric insulator [12]. Soft ferrites are ferrimagnetic oxides of iron combined with divalent transition metals like nickel, cobalt, manganese, zinc, or magnesium. The addition of such metals in various proportions and combinations, together with the fabrication process's temperature, allows the creation of many different final materials whose frequency-dependent properties may vary widely. For an overview on the state-of-the-art on microwave magnetic media, with emphasis on ferrite materials, the reader may refer to [7]–[16].

Ferromagnetic and ferrimagnetic materials have a permeability that can be very high at dc, but decrease quickly with increasing frequency according to Snoek's law [17], [18] until the relative permeability is ordinarily in the 1–10 range at 1 GHz. Nonetheless, according to [15], thin films of ferromagnetic material can produce far higher microwave permeability than predicted by Snoek's law (valid for bulk materials). Also, in a data sheet, concerning an NiZn soft ferrite specimen UR1.5K manufactured by UNIMAGNET, an initial relative permeability of 1.5×10^3 is reported for operation up to 0.1 GHz.

In short, it seems that future advances in magnetic materials do not allow to definitely rule out the possibility of high permeability at microwave frequencies.

VIII. Conclusion

A novel theoretical development aimed at the analysis of MGTLs was established. An MGTL is a transmission line, carrying a magnetic flux, made of two parallel magnetic wires of high permeability immersed in an insulating dielectric medium—it is the dual counterpart of familiar ELTLs. In the transverse plane of an MGTL, the H-field lines are open lines starting and ending at the magnetic wires, conversely, the E-field lines are closed lines embracing the magnetic wires. The field structure observed in an ELTL and in an MGTL ensures that if those two lines run parallel to each other, they will not couple; crosstalk will not exist.

In this paper, the frequency-domain propagation equations governing the longitudinal variation of the magnetic voltage and the longitudinal variation of the magnetic flux were established and solved. The propagation constant and characteristic wave impedance of the MGTL were obtained and further simplified for the case of small losses.

This paper is purely theoretical. Applications of MGTLs must be analyzed in a future step, where the key problem will be the correct specification of the frequency-dependent complex permeability and complex permittivity of the ferrite medium to be used for the materialization of the magnetic wires, whether they take the shape of cylinders, strips, or any other shape.

Appendix A

Skin-effect theory for solid cylindrical electric wires carrying a time–harmonic axial current leads to the following well-known expression for the wire's pul impedance [5]:

$$\overline{Z}_{\rm skin}(\omega) = R_{\rm DC}\overline{\kappa}_E \frac{J_0(\overline{\kappa}_E)}{2J_1(\overline{\kappa}_E)} \tag{A1}$$

where J_0 and J_1 are the Bessel functions of the first kind of orders 0 and 1, respectively, $R_{\rm DC} = 1/(\sigma_E S_e)$ is the pul wire resistance at $\omega = 0$, and $\overline{\kappa}_E$ is a frequency-dependent dimensionless complex given by

$$\overline{\kappa}_E(\omega) = \sqrt{-j\omega\mu_E(\sigma_E + j\omega\varepsilon_E)} \times r_w \tag{A2}$$

where r_w denotes the wire radius. Ordinarily, for frequencies up into the optical range, the term $j\omega\varepsilon_E$ is discarded since it is negligibly small compared to σ_E.

The procedure (integration of Maxwell's equations) that is used to derive the result in (A1) can be followed to obtain the pul complex reluctance of a cylindrical magnetic wire carrying a time–harmonic axial magnetic flux

$$\overline{R}m_{\rm skin}(\omega) = Rm_{\rm DC}\overline{\kappa}_M \frac{J_0(\overline{\kappa}_M)}{2J_1(\overline{\kappa}_M)} \tag{A3}$$

where

$$Rm_{\rm DC} = \frac{1}{S_m(\mu_M)_{\rm DC}} \tag{A4}$$

and

$$\overline{\kappa}_M(\omega) = \sqrt{-j\omega\mu_M(\sigma_M + j\omega\varepsilon_M)} \times r_w. \tag{A5}$$

The result in (A5) can be generalized to accommodate a complex frequency-dependent permeability $\overline{\mu}_M(\omega)$, and a complex frequency-dependent permittivity $\overline{\varepsilon}_M(\omega)$, which, formally, can aggregate the wire's conductivity

$$\begin{cases} \overline{\mu}_M(\omega) = \mu'_M - j\mu''_M \\ \overline{\varepsilon}_M(\omega) = \varepsilon'_M - j\left(\varepsilon''_M + \sigma_M/\omega\right). \end{cases} \tag{A6}$$

Substituting (A6) into (A5), we will get

$$\overline{\kappa}_M(\omega) = \omega\sqrt{\overline{\mu}_M(\omega)\overline{\varepsilon}_M(\omega)} \times r_w. \tag{A7}$$

Substituting (A7) into (A3), the generalized form of the pul complex reluctance of the wire is obtained. By using the complex Poynting theorem [5], it can be shown that while the real part of $\overline{R}m_{\rm skin}$ is associated to magnetic and electric energy

storage inside the magnetic wire, the imaginary part of $\overline{R}m_{\rm skin}$ is associated to wire losses due to conduction, polarization, and magnetization mechanisms

$$\begin{cases} \mathrm{Re}(\overline{R}m_{\rm skin}) = 2\dfrac{(W_m)_{\rm av} - (W_e)_{\rm av}}{\phi^2_{\rm rms}} \\ \mathrm{Im}(\overline{R}m_{\rm skin}) = \dfrac{P_{\rm loss}}{\omega\phi^2_{\rm rms}}. \end{cases} \tag{A8}$$

Note, from above, that while $\mathrm{Im}(\overline{R}m_{\rm skin})$ is always a positive quantity, $\mathrm{Re}(\overline{R}m_{\rm skin})$ can be positive, negative, or zero, depending on the frequency.

At last, we emphasize that the concept of magnetic reluctance belongs with linear systems, and therefore, the magnetic flux in the wire must be sufficiently weak in order to avoid magnetic saturation.

Appendix B

Each MGTL wire can be viewed as an aggregate of filamentary wires. Due to linearity, the electromagnetic field of the MGTL is the result of the superposition of the effects produced by all the filaments.

Consider one such filament carrying an elemental magnetic flux $\Delta\phi$ flowing opposite to the z-direction. In the transverse plane, the electric induction field is azimuthal, $\overline{\mathbf{E}} = \overline{E}\vec{e}_\theta$, and the gradient magnetic field is radial $\overline{\mathbf{H}} = \overline{H}\vec{e}_r$, both field strengths decreasing with r. From (10) and (11), it follows:

$$\begin{cases} 2\pi r\overline{E} = j\omega\Delta\overline{\phi} \\ \overline{E} = j\omega\dfrac{\Delta\overline{\phi}}{\xi_E} \end{cases} \rightarrow \xi_E = 2\pi r \tag{B1}$$

and, from (15), making $ds_H = dr$, we find

$$(g_M)_{\rm filament} = \int_{P_1}^{P_2} \frac{dr}{\xi_E} = \int_{P_1}^{P_2} \frac{dr}{2\pi r} \tag{B2}$$

where $P_1(r = r_1)$ and $P_2(r = r_2)$ are points belonging to the same transverse plane. From (17) and (18), making $ds_H = dr$, and enforcing $r\overline{H} =$ constant, it follows:

$$\begin{cases} \overline{U} = \int_{P_1}^{P_2} \overline{H}dr \\ \overline{H} = \dfrac{\overline{U}}{\xi_H} \end{cases} \rightarrow \xi_H = \left(r\int_{P_1}^{P_2} \frac{dr}{r} \right) \tag{B3}$$

at last, from (21a), making $ds_E = rd\theta$, we find

$$(g'_M)_{\rm filament} = \int_0^{2\pi} \frac{rd\theta}{\xi_H} = \left(\int_{P_1}^{P_2} \frac{dr}{2\pi r} \right)^{-1} \tag{B4}$$

showing, for homogeneous media, that $g'_M = 1/g_M$, as asserted in (22).

References

[1] J. B. Faria, "Poynting vector flow analysis for contactless energy transfer in magnetic systems," *IEEE Trans. Power Electron.*, vol. 27, no. 10, pp. 4292–4300, Oct. 2012.

[2] Q. A. Kerns, "Transient-supressing magnetic transmission line," US Patent 3 376 523, Apr. 2, 1968.

[3] J. B. Faria, ""Dispositivo Formado por uma Linha Magnética de Transmissão Para uso em Circuitos Integrados Para Aplicações na Tecnologia Terahertz" (magnetic transmission line device for terahertz integrated circuits)," Portugal Patent PT 106056, Dec. 12, 2011.

[4] J. B. Faria, "The role of Poynting's vector in polyphase power calculations," *Eur. Trans. Electric. Power*, vol. 19, pp. 683–688, 2009.

[5] J. B. Faria, *Electromagnetic Foundations of Electrical Engineering*. Chichester, U.K.: Wiley, 2008.

[6] P. Magnusson, G. Alexander, V. Tripathi, and A. Weisshaar, *Transmission Lines and Wave Propagation*, 4th ed. Boca Raton, FL: CRC, 2001.

[7] E. F. Schloemann, "Behavior of ferrites in the microwave frequency range," *J. Phys.*, vol. 32, pp. 441–443, 1971.

[8] G. F. Dionne, "A review of ferrites for microwave applications," *Proc. IEEE*, vol. 63, no. 5, pp. 777–789, May 1975.

[9] V. Voronkov, "Microwave ferrites: The present and the future," *J. Phys. IV*, vol. 7, pp. 35–38, 1997, Colloq. C1.

[10] G. F. Dionne, "Properties of ferrites at low temperatures," *J. Appl. Phys.*, vol. 81, pp. 5064–5069, 1997.

[11] E. F. Schloemann, "Advances in ferrite microwave materials and devices," *J. Magn. Magn. Mater.*, vol. 209, pp. 15–20, 2000.

[12] M. P. Horvath, "Microwave applications of soft ferrites," *J. Magn. Magn. Mater.*, vol. 215/216, pp. 171–183, 2000.

[13] O. Acher and A. L. Adenot, "Bounds on the dynamic properties of magnetic materials," *Phys. Rev. B, Condens. Matter*, vol. 62, pp. 11 324–11 327, 2000.

[14] J. D. Adam, L. E. Davis, G. F. Dionne, E. F. Schloemann, and S. N. Stitzer, "Ferrite devices and materials," *IEEE Trans. Microw. Theory Tech.*, vol. 50, no. 3, pp. 721–737, Mar. 2002.

[15] K. N. Rozanov, I. T. Iakubov, A. N. Lagarkov, S. A. Maklakov, A. V. Osipov, D. A. Petrov, I. A. Ryzhikov, M. V. Sedova, and S. N. Starostenko, "Laminates of thin ferromagnetic films for microwave applications," in *Proc. MSMW Symp.*, Kharkov, Ukraine, Jun. 2007, pp. 168–173.

[16] A. N. Lagarkov and K. N. Rozanov, "High-frequency behavior of magnetic composites," *J. Magn. Magn. Mater.*, vol. 321, pp. 2082–2092, 2009.

[17] Y. Liu, D. Shindo, and D. J. Sellmyer, *Handbook of Advanced Magnetic Materials*. New York: Springer, 2005.

[18] G. F. Dionne, *Magnetic Oxides*. New York: Springer, 2009.

J. A. Brandão Faria (M'87–SM'90–F'11) received the Ph.D. degree in electrical engineering from the Instituto Superior Técnico, Technical University of Lisbon, Lisbon, Portugal, in 1986.

Since 1994, he has been a Full Professor of electrical engineering with the Instituto Superior Técnico, Technical University of Lisbon. He has authored or coauthored over 100 papers appearing in major peer-reviewed periodicals. He authored *Electromagnetic Foundations of Electrical Engineering* (Wiley, 2008), *Optica* (Editorial Presença, 1995), and *Multiconductor Transmission-Line Structures* (Wiley, 1993). His current research areas of interest include electromagnetic-field problems, applied electromagnetics, power lines, and wave propagation phenomena in multiconductor transmission lines.

Miguel P. Pires received the Diploma degree in electrical engineering from the Instituto Superior Técnico, Technical University of Lisbon, Lisbon, Portugal, in 2000, and is currently working toward the Master's degree in electrical engineering at the Instituto Superior Técnico, Technical University of Lisbon. His thesis concerns MGTLs.